Phase space geometry and stochasticity thresholds in Hamiltonian dynamics

Monica Cerruti-Sola* and Marco Pettini†
Osservatorio Astrofisico di Arcetri, Largo E. Fermi 5, 50125 Firenze, Italy
and Istituto Nazionale di Fisica della Materia, UdR di Firenze, Frienze, Italy

E. G. D. Cohen‡
The Rockefeller University, 1230 York Avenue, New York, New York 10021-6399
(Received 10 May 2000)

Results of numerical computations of the largest Lyapunov exponent $\lambda_1(\varepsilon,N)$ as a function of the energy density ε and the number of particles N are here reported for a Fermi-Pasta-Ulam $\alpha+\beta$ model. These results show the coexistence at large N of two thresholds: a stochasticity threshold, found before for the α model alone, and a strong stochasticity threshold (SST), found before for the β model alone. Although this coexistence may seem at first sight plausible, it is not obvious *a priori* that the $\alpha+\beta$ model superimposes properties of the α and β models independently. The main point of this paper, however, is a geometric characterization of the SST via the mean curvature of the constant energy hypersurfaces in the phase space of the model and the characteristic decay time of its time autocorrelation function $\tau_c(\varepsilon,N)$, which correlates with that of $\lambda_1(\varepsilon,N)$ for fixed N. This appears to provide important information on the very complicated geometry of the phase space of this simple solidlike model.

PACS number(s): 05.20.−y, 05.45.−a

Since the seminal study by Fermi and collaborators [1] of the dynamics of anharmonically perturbed chains of harmonic oscillators, a wealth of investigations has been performed. The overwhelming majority of these investigations, following Fermi *et al.*, have dealt with the problem of the redistribution of energy—initially concentrated in a few normal modes—among all the normal modes, i.e., the problem of the approach to equipartition and equilibrium.

However, in this paper we concentrate on a different problem, namely, what is the nature of the phase space, and in particular of the constant energy surfaces, which represent these equilibrium states? Thus, instead of considering the relaxation properties of *nonequilibrium initial* states, which are still addressed in the very recent literature [2], we want here to investigate the nature of the *final equilibrium* states, in particular their geometric structure. This was made possible by a combination of the previously separately considered Fermi-Pasta-Ulam (FPU) α and FPU β models.

In the FPU α model [3], we discovered the existence of a stochasticity threshold (ST), at an energy density ε, below which the dynamics appears to be regular. However, the dynamics of this model is stable only if ε does not exceed an upper limit $\varepsilon \simeq 0.5$. Earlier in [4,5], the FPU β model was considered, where a strong stochasticity threshold (SST) was found, above which the dynamics appears to be strongly chaotic. By combining these two models into the FPU $\alpha+\beta$ model, we are able to obtain a much more complete and possibly generic picture of the dynamical behavior of these systems in that part of their phase space that corresponds to equilibrium for all $0.3<\varepsilon<9\times10^4$ and $8\leqslant N\leqslant 1024$.

The FPU $\alpha+\beta$ model is described by the Hamiltonian

$$H(\mathbf{p},\mathbf{q})=\sum_{k=1}^{N}\left[\frac{1}{2}p_k^2+\frac{1}{2}(q_{k+1}-q_k)^2+\frac{\alpha}{3}(q_{k+1}-q_k)^3+\frac{\beta}{4}(q_{k+1}-q_k)^4\right], \tag{1}$$

where the particles have unit mass and unit harmonic coupling constant and the end points are fixed ($q_1=q_{N+1}=0$). We can think of Eq. (1) as a truncated power series expansion of a Toda potential [6], which, in the same units, is described by the Hamiltonian $H(\mathbf{p},\mathbf{q})=\Sigma_{k=1}^{N}\frac{1}{2}p_k^2+(1/4\alpha^2)\{\exp[-2\alpha(q_{k+1}-q_k)]+2\alpha(q_{k+1}-q_k)-1\}$, where the α is chosen equal to that in Eq. (1) and $\beta=\frac{2}{3}\alpha^2$. This choice leads to a potential very close to interatomic potentials of the Morse or Lennard-Jones type in solids in a suitably restricted range of ε.

We have focused on chaoticity properties of generic trajectories in the equilibrium state, as a function of the energy density $\varepsilon=E/N$ and N. To that end, we have integrated Hamilton's equations of motion derived from Eq. (1) with $\alpha=0.25$ and $\beta=\frac{2}{3}\alpha^2$, together with the standard tangent dynamics equations. The method is described in [3]. In what follows, $t=1$ corresponds to $1/\pi$ times the period of the fastest harmonic mode [3].

The largest Lyapunov exponents $\lambda_1(\varepsilon,N)$ have been determined at different energy densities ε and for different values of $N=8,16,32,64,128,512,1024$. Random initial conditions have been chosen, i.e., $\{q_i(0)=0,p_i(0)=r_i\}$, $i=1,\ldots,N$, where the numbers r_i are Gauss-distributed random numbers with zero mean and variance $\sqrt{2\varepsilon}$. This can be considered as a generically close to equilibrium initial state, as has been investigated already in previous papers [3–5]. As an additional check, single mode excitations have also been

*Email address: mcerruti@arcetri.astro.it
†Also at INFN Sezione di Firenze, Italy. Email address: pettini@arcetri.astro.it
‡Email address: egdc@rockvax.rockefeller.edu

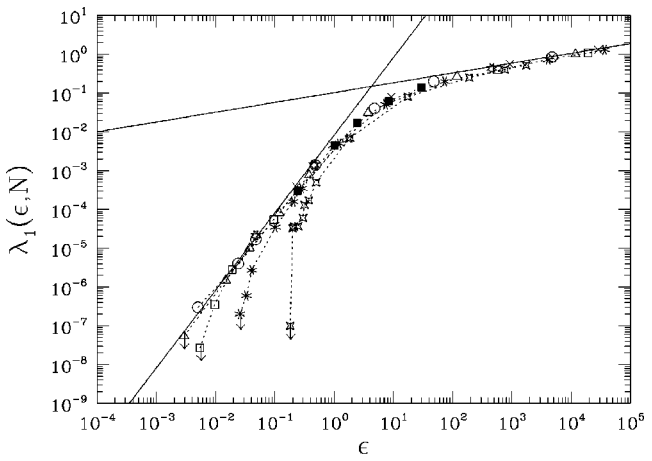

FIG. 1. The largest Lyapunov exponents $\lambda_1(\varepsilon,N)$ are shown for different values of the energy density ε for various values of N. Starlike squares refer to $N=8$, asterisks to $N=16$, open squares to $N=32$, open triangles to $N=64$, open circles to $N=128$, starlike polygons to $N=512$, and crosses to $N=1024$. Full squares refer to $N=32$ and excitation amplitudes A ranging from 5 to 50. Solid lines are the asymptotic scalings ε^2 and $\varepsilon^{1/4}$ at low and high energy density, respectively.

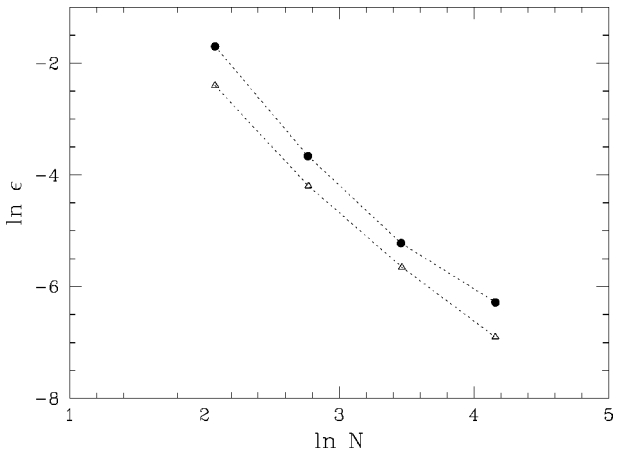

FIG. 2. The ε values of the stochasticity thresholds are plotted for different values of N ranging from 8 to 64 and compared with those of the FPU α model [3] (open triangles).

considered in this paper for $N=32$ and $\varepsilon=0.3$ to 3 (see Fig. 1), i.e., initial $q_i(0)=A\sin(2\pi i/N)$ and $p_i(0)=0$ for $i=1,\ldots,N=32$, which confirmed again the independence of the final equilibrium state of the initial conditions.

The results of the computations are reported in Fig. 1, where $\lambda_1(\varepsilon,N)$ is plotted as a function of ε. We have used $t=4.3\times10^8$ as an upper bound for the integration time. If, after such a long time, no convergence in time of λ_1 to a positive asymptotic value could be observed, then the values of λ_1 at $t=4.3\times10^8$ (the lowest points of the broken lines in Fig. 1, marked by arrows) are taken as upper bounds for the Lyapunov exponents. For $N\geqslant128$, no reasonable upper bound of λ_1 could be obtained, even with such a long integration time. In fact, the FPU $\alpha+\beta$ model with $\beta=\frac{2}{3}\alpha^2$ is a fourth-order approximation of the Toda lattice model and at low ε the system is very close to integrability.

The patterns of $\lambda_1(\varepsilon,N)$ reported in Fig. 1 display some remarkable features. For small values of the energy density, there is a sudden drop of λ_1 which, in close analogy with Ref. [3], allows us to define a ST below which we can assume that the overwhelming majority of trajectories in phase space are regular. This ST moves to smaller and smaller values of ε as N is increased. At each N, the value of ε at the lowest point on each curve $\lambda_1(\varepsilon,N)$ has been taken as an estimate for the ε value of the ST. In Fig. 2, these threshold values are plotted vs N, together with those found for the FPU α model [3]; their increase at any given value of N signals that the FPU $\alpha+\beta$ model is closer to integrability than the FPU α model. The physical relevance of the vanishing of the ST with increasing N is that the existence of regular regions below a critical energy density does not constitute a problem for equilibrium statistical mechanics of macroscopic solidlike systems, if the one-dimensional FPU $\alpha+\beta$ behavior is typical in general.

Around $\varepsilon\simeq0.8$, a ''knee'' is observed in the pattern $\lambda_1(\varepsilon,N)$ (Fig. 1), due to a crossover between two power law behaviors, $\sim\varepsilon^2$ at small ε and $\sim\varepsilon^{1/4}$ at large ε, where the latter has been attributed to the existence of a SST [4,5]. This crossover is presumably a signature of a transition from weak to strong chaos, as already discussed in [4,5]. Unlike the ST, the SST appears to be a generic property of Hamiltonian systems with a large number ($N\gg2$) of degrees of freedom [7–18]: it is stable with N and it is independent of the initial conditions.

We now report a characterization of the SST within a geometric framework [19], which throws an entirely different light on the nature of the SST. In particular, we are able to find a geometric quantity, the mean curvature of the constant energy hypersurfaces Σ_E in the phase space of the system, whose behavior correlates with that of $\lambda_1(\varepsilon,N)$. In fact, a standard way to investigate the geometry of a hypersurface Σ^m is to study the way in which it curves around in R^{m+1} [20], which is measured by the way the normal direction changes as one moves from point to point on the surface. The rate of change of the normal direction to the hypersurface $\mathbf{N}$ at a point $x\in\Sigma_E$ is described by the shape operator $L_x(\mathbf{v})=-\nabla_{\mathbf{v}}\mathbf{N}$, where $\mathbf{v}$ is a tangent vector at x and $\nabla_{\mathbf{v}}$ is the directional derivative of the unit normal $\mathbf{N}$, so that $L_x(\mathbf{v})=-(\nabla N_1\cdot\mathbf{v},\ldots,\nabla N_{m+1}\cdot\mathbf{v})$. Since L_x is a mapping of the tangent space at x into itself, there are m independent eigenvalues [20] $\kappa_1(x),\ldots,\kappa_m(x)$, which are called the principal curvatures of Σ^m at x. Their sum is the so-called mean curvature: $M_1(x)=(1/m)\Sigma_{i=1}^m\kappa_i(x)$, the trace of $L_x(\mathbf{v})$. It can be shown [21] that the mean curvature—replacing m by $2N-1$, if N is the number of degrees of freedom—is given by

$$M_1(x)=-\frac{1}{2N-1}\nabla\cdot\left(\frac{\nabla H(x)}{\|\nabla H(x)\|}\right), \tag{2}$$

where $\nabla H/\|\nabla H\|$ is the unit normal to Σ_E at a given point $x=(p_1,\ldots,p_N,q_1,\ldots,q_N)$.

The autocorrelation functions $\Gamma(\tau)=\langle\delta M_1(t+\tau)\,\delta M_1(t)\rangle_t$ of the time series of the values $M_1[x(t)]$ at the points of the hypersurface visited by the phase space trajectory can provide a good indication of how the ''covering'' of a hypersurface Σ_E by the motion of a phase space trajectory on it proceeds and is affected by the geometry and topology of the Σ_E itself. A number of M_1 autocorrelation

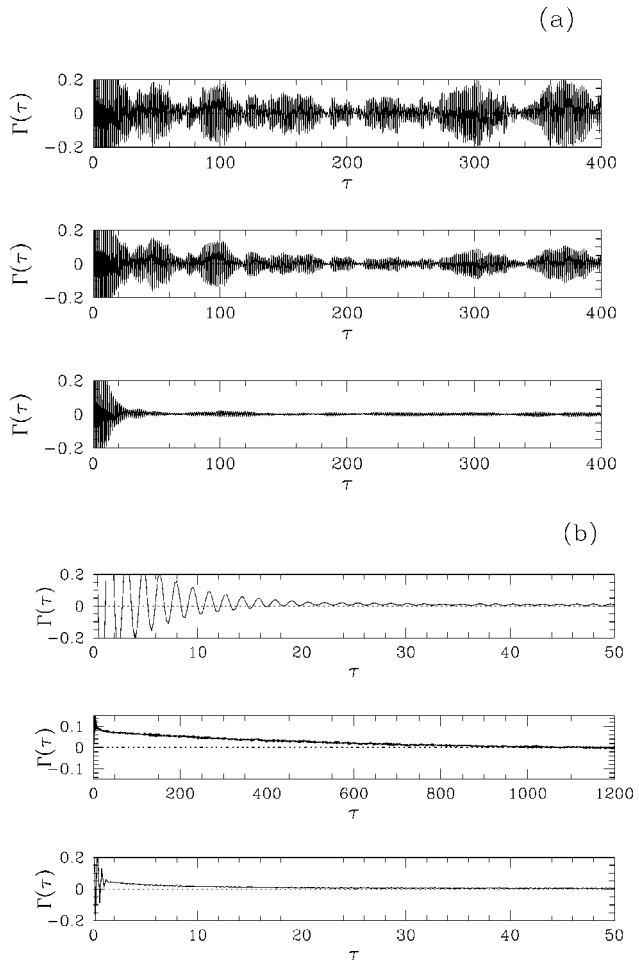

FIG. 3. The mean curvature autocorrelation functions $\Gamma(\tau)$ are shown for $N=1024$ and for different values of the energy density: (a) $\varepsilon=0.931\times10^{-6}$,0.009 31,0.0931 (from top to bottom); (b) $\varepsilon=0.279$,1.397,9.314 (from top to bottom).

functions $\Gamma(\tau)$ has been computed for $N=8,\ldots,1024$ and for different values of ε. Figures 3(a) and 3(b) show some examples of these functions plotted versus time for $N=1024$ and different energy densities. Above $\varepsilon\simeq0.3$, the autocorrelation functions show a short initial regime of fast decay, followed by a slow decay, which gives rise to a ''tail.'' By defining an autocorrelation time τ_c as the time of the first intercept of $\Gamma(\tau)$ with the level 0.01, we have obtained $\tau_c(\varepsilon)$. The behavior of $\tau_c(\varepsilon)$ is reported in Fig. 4 for different values of N. Below $\varepsilon\simeq0.3$, the patterns of $\Gamma(\tau)$, even at $\tau\sim3000$, do not allow an unambiguous definition of τ_c. The $\tau_c(\varepsilon)$ are sharply peaked around $\varepsilon\simeq0.8$. By superimposing the plot of λ_1 on the plot of τ_c, as is done in Fig. 5, one observes that the peak of the decay times $\tau_c(\varepsilon)$ at $\varepsilon\simeq0.8$ corresponds to the region where $\lambda_1(\varepsilon)$ starts to deviate from its ε^2 behavior, i.e., from that in the weakly chaotic regime. The peak shown by $\tau_c(\varepsilon)$ provides a more precise definition of the SST and of its value in terms of the energy density than obtained by using the criterion of [4,5], i.e., the crossover between the two asymptotic ε scalings of λ_1.

It is worth mentioning that the above reported related behavior of $\Gamma(\tau)$ and $\tau_c(\varepsilon)$ has so far only been found for the observable M_1. Attempts to show through other observables energy dependent memory effects along phase space trajectories, sensitive to the SST, have not yet succeeded. Thus, the observed patterns of $\Gamma(\tau)$ and $\tau_c(\varepsilon)$ seem closely related to the geometric landscapes of the energy surfaces Σ_E and to the way they are visited by the phase space trajectories on them.

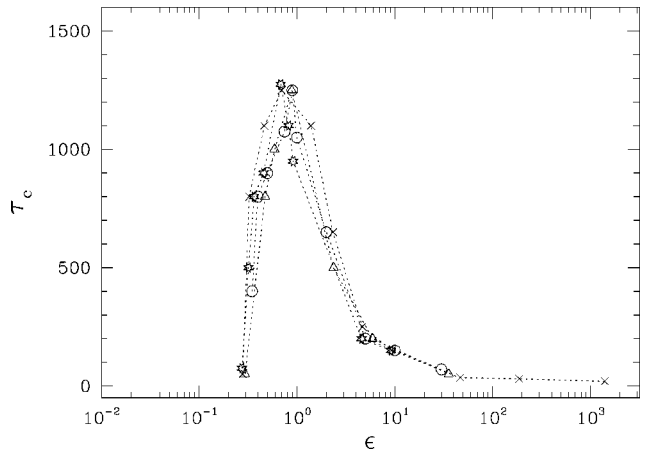

FIG. 4. The decay times τ_c of the $\Gamma(\tau)$ are shown for different values of ε. Open triangles refer to $N=64$, open circles to $N=128$, starlike polygons to $N=512$, and crosses to $N=1024$.

We now make an attempt to deduce physically from the $\tau_c(\varepsilon)$ curve the possible phase space geometry of the system. One could think of the energy surfaces Σ_E as rough bumpy surfaces as indicated by the nonconstancy of M_1. Figures 4 and 5 show that at $\varepsilon\leqslant0.3$ $\tau_c\simeq0$. This could perhaps be understood by noting that the Σ_E landscape will then be rather similar to that of a collection of harmonic oscillators. Therefore, during observation times much shorter than λ_1^{-1} [as in Fig. 3(a)], $\Gamma(\tau)$ will reflect the interplay of an almost regular dynamics on a relatively smooth surface with a uniform distribution of bumps on Σ_E over which the phase point ''glides'' easily. This might well be compatible with the nondecaying patterns of $\Gamma(\tau)$ and a $\tau_c\simeq0$. For $0.3<\varepsilon<0.8$, $\tau_c(\varepsilon)$ climbs steeply to about 1300, after which it decays somewhat less steeply to about $\tau_c\simeq200$ at $\varepsilon=4$ to 5. The steep rise in τ_c for $0.3<\varepsilon<0.8$ seems to indicate the

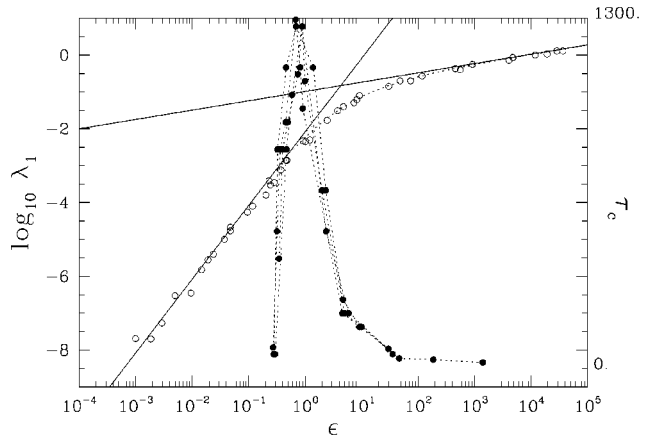

FIG. 5. The decay times τ_c of the $\Gamma(\tau)$ (full circles) are plotted together with the largest Lyapunov exponents (open circles) versus ε, for various values of N; the solid lines are the power laws ε^2 and $\varepsilon^{1/4}$ of their asymptotic behaviors, respectively. Note the sharp maximum at $\varepsilon\simeq0.8$.

appearance of weak chaos when the landscape of Σ_E is much less smooth and much bumpier than for $\varepsilon<0.3$. This would allow a quasitrapping-related ''sticky'' intermittent motion and a very considerable lengthening of $\tau_c(\varepsilon)$. The subsequent decay of $\tau_c(\varepsilon)$ for $0.8<\varepsilon<4$ shows that this is short lived and that, when the $\lambda_1(\varepsilon)$ curve really starts to bend over at $\varepsilon\simeq 4$, and strong chaos begins to develop more and more, the τ_c drastically decreases again, since the now emerging strong chaos, even if still weak, destroys the quasitrapping. This implies a strongly erratic motion of the phase point on Σ_E, which has now a highly irregular, bumpy landscape, compatible with a rapidly decaying $\Gamma(\tau)$ as well as a decreasing τ_c with increasing ε. The slower decay for $4<\varepsilon<35$ occurs in the middle of the ε^2 to $\varepsilon^{1/4}$ transition and may be influenced by a balancing of the two different physical mechanisms responsible for the weak chaos behavior (ε^2) and the strong chaos behavior ($\varepsilon^{1/4}$). Finally, the very slow decay of $\tau_c(\varepsilon)$ for $\varepsilon>35$ might be due to the appearance of large scale inhomogeneities in the distribution of bumps on Σ_E. In fact, we might speculate the existence of a valley with very irregularly distributed bumps in it, in which the phase point chaotically wiggles around. The small, yet sizable memory effect, as signaled by the long tail of $\Gamma(\tau)$ for $\varepsilon>35$, could therefore reflect the presence of some coherence in the large scale arrangement of the bumps on Σ_E.

In this sense, the geometric framework based on the mean curvature of Σ_E, $M_1(x)$, allows a geometric ''exploration'' of the equilibrium phase space of the FPU $\alpha+\beta$ model, and deduction of some possible salient geometric features of the immensely complicated hypersurfaces in configuration space of this relatively simple model. To what extent this picture is correct for this model and even if it is, is generic for solidlike Hamiltonian systems in general, remain interesting open questions.

This work was done during a visit of E.G.D.C. to the Research Unit of Firenze of the INFM. It was financed by the IS Sabbatical Program of the theoretical division—Sezione G—of the INFM, which is hereby gratefully acknowledged. E.G.D.C. is also indebted to the Office of Basic Engineering Sciences of the U.S. Department of Energy, under Grant No. DE-FG 02-88-ER 13847.

[1] E. Fermi, J. Pasta, and S. Ulam, Los Alamos Report LA-1940, 1955, in *Collected Papers of Enrico Fermi*, edited by E. Segré (University of Chicago Press, Chicago, 1965), Vol. 2, p. 978.

[2] H. Kantz, R. Livi, and S. Ruffo, J. Stat. Phys. **76**, 627 (1994); J. De Luca, A.J. Lichtenberg, and M.A. Lieberman, Chaos **5**, 283 (1995); D. Shepelyansky, Nonlinearity **10**, 133 (1997); T. Dauxois, S. Ruffo, A. Torcini, and T. Cretegny, Physica D **121**, 109 (1998); Ya. A. Kosevich, and S. Lepri, Phys. Rev. B **61**, 99 (2000); K. Ullmann, A.J. Lichtenberg, and G. Corso, Phys. Rev. E **61**, 2471 (2000).

[3] L. Casetti, M. Cerruti-Sola, M. Pettini, and E. G. D. Cohen, Phys. Rev. E **55**, 6566 (1997).

[4] M. Pettini and M. Landolfi, Phys. Rev. A **41**, 768 (1990).

[5] M. Pettini and M. Cerruti-Sola, Phys. Rev. A **44**, 975 (1991).

[6] A.J. Lichtenberg and M.A. Lieberman, *Regular and Chaotic Dynamics* (Springer, New York, 1991).

[7] This transition was already implied by P. Bocchieri, A. Scotti, B. Bearzi, and A. Loinger, Phys. Rev. A **2**, 2013 (1970). The authors interpreted their results as a transition from regular to chaotic motion and not as a transition from weak to strong chaos, because at that time computers did not permit sufficiently long and accurate measurements of very small Lyapunov exponents, necessary to detect the existence of a weakly chaotic regime.

[8] P. Butera and G. Caravati, Phys. Rev. A **36**, 962 (1987).

[9] D. Escande, H. Kantz, R. Livi, and S. Ruffo, J. Stat. Phys. **76**, 539 (1987).

[10] S. Isola, R. Livi, and S. Ruffo, Europhys. Lett. **3**, 407 (1987).

[11] L. Casetti, C. Clementi, and M. Pettini, Phys. Rev. E **54**, 5969 (1996).

[12] L. Caiani, L. Casetti, C. Clementi, and M. Pettini, Phys. Rev. Lett. **79**, 4361 (1997).

[13] V. Constantoudis and N. Theodorakopoulos, Phys. Rev. E **55**, 7612 (1997).

[14] K. Yoshimura, Physica D **104**, 148 (1997).

[15] L. Caiani, L. Casetti, and M. Pettini, J. Phys. A **31**, 3357 (1998).

[16] L. Caiani, L. Casetti, C. Clementi, G. Pettini, M. Pettini, and R. Gatto, Phys. Rev. E **57**, 3886 (1998).

[17] M.-C. Firpo, Phys. Rev. E **57**, 6599 (1998).

[18] C. Giardinà and R. Livi, J. Stat. Phys. **91**, 1027 (1998).

[19] M. Cerruti-Sola, C. Clementi, and M. Pettini, Phys. Rev. E **61**, 5171 (2000).

[20] J.A. Thorpe, *Elementary Topics in Differential Geometry* (Springer, New York, 1979), Chaps. 9 and 12.

[21] M.P. Do Carmo, *Riemannian Geometry* (Birkhäuser, Boston, 1992), p. 142.